JACC: CARDIOVASCULAR IMAGING
VOL. 3, NO. 12, 2010
© 2010 BY THE AMERICAN COLLEGE OF CARDIOLOGY FOUNDATION
ISSN 1936-878X/$36.00
PUBLISHED BY ELSEVIER INC.
DOI:10.1016/j.jcmg.2010.09.017

Contrast-Enhanced Ultrasound Imaging Detects Intraplaque Neovascularization in an Experimental Model of Atherosclerosis

Chiara Giannarelli, MD, PhD,* Borja Ibanez, MD,* Giovanni Cimmino, MD,* Josè M. Garcia Ruiz, MD,* Francesco Faita, MSc,† Elisabetta Bianchini, MSc,† M. Urooj Zafar, MBBS,* Valentin Fuster, MD, PhD,* Mario J. Garcia, MD,‡ Juan J. Badimon, PhD*

New York and Bronx, New York; and Pisa, Italy

OBJECTIVES The aims of this study were to investigate the feasibility of contrast-enhanced ultrasound (CEU) imaging for in vivo visualization of intraplaque neovascularization and to correlate the in vivo observations with histological assessment of neovessel density and plaque composition in an experimental animal model of advanced atherosclerosis.

BACKGROUND Recent evidence has linked plaque angiogenesis with enhanced atherosclerotic plaque progression and vulnerability. Increased neovascularization has been detected in ruptured human lesions and is associated with clinical manifestations of plaque rupture.

METHODS Advanced aortic atherosclerosis was induced in New Zealand white rabbits (n = 21; high cholesterol–rich diet/double-balloon aortic denudation). Animals underwent standard and CEU imaging at the end of the atherosclerosis induction period. Six age-matched animals served as control subjects. Within 24 h, animals were euthanized and aortas processed for histopathological evaluation of plaque composition and neovascularization. Imaged plaques were classified as contrast enhanced (CE) positive or CE negative, according to their contrast enhancement on CEU imaging. The lesions were also classified as class III (predominantly echogenic) or class II (predominantly echolucent), according to their echogenicity on non-CEU images.

RESULTS No contrast enhancement was observed in control animals. In atherosclerotic animals, class III lesions showed an increased contrast enhancement compared with class II lesions and CE-positive lesions showed greater neovascularization than CE-negative plaques. Macrophage density, but not smooth muscle cell density, was significantly higher in CE-positive than CE-negative lesions. As expected, class III lesions showed increased macrophage density compared with class II plaques. Intraplaque neovessel density at histology was significantly higher in CE-positive than in CE-negative lesions. Class III plaques showed a significantly higher neovessel density compared with class II lesions. A strong correlation between intraplaque neovessels and contrast enhancement was found.

CONCLUSIONS CEU imaging is a feasible noninvasive imaging modality to evaluate intraplaque neovascularization. A noninvasive imaging modality to assess lesion neovascularization could be of great importance to identify vascularized, "high-risk" lesions before rupture. (J Am Coll Cardiol Img 2010;3: 1256–64) © 2010 by the American College of Cardiology Foundation

From the *AtheroThrombosis Research Unit, Cardiovascular Institute, Mount Sinai School of Medicine, New York, New York; †IFC, CNR, Pisa, Italy; and the ‡Division of Cardiology, Montefiore Medical Center, Einstein School of Medicine, Bronx, New York. The authors have reported that they have no relationships to disclose.

Manuscript received August 5, 2010; accepted September 16, 2010.

Cardiovascular events, resulting from plaque rupture and occlusive atherothrombosis, are still the number one cause of death in the Western countries, with approximately 1.2 million heart attacks and 750,000 strokes afflicting the American population each year (1). Accumulating evidence has linked plaque angiogenesis with enhanced lesion progression and vulnerability (2,3). Increased neovascularization has been detected in ruptured human aortic plaques and is frequently associated with pathological signs of plaque vulnerability such as intraplaque hemorrhage and thin-cap fibroatheromas (4–9). Therefore, the availability of a noninvasive technique capable of reliably identifying lesion neovascularization could be particularly attractive for early detection of high-risk, prone-to-rupture plaques before the occurrence of clinical events.

Contrast-enhanced ultrasound (CEU) imaging has been proposed as a feasible and effective technique to detect neovascularization of human atherosclerotic plaque (10–12). The direct visualization of contrast microbubbles within plaque neovascularization was previously described (13,14). These findings were confirmed by a more recent study correlating CEU imaging of carotid arteries with the presence and degree of intraplaque neovascularization as corroborated by histology of the same lesions (15). Visualization of adventitial vasa vasorum in carotid arteries in patients with or without carotid atherosclerosis was recently reported using CEU imaging (16). Despite the promising potential application of CEU imaging in the clinical setting, few studies have included histological validation of the imaging results. The ones that did were limited to high-risk lesions collected from patients undergoing surgical procedures. Moreover, the fact that carotid endarterectomy specimens do not include the whole arterial wall limits the histological evaluation to intraplaque neovascularization and may exclude the assessment of adventitial vasa vasorum.

The aims of this study were to investigate the feasibility of CEU imaging for in vivo visualization of intraplaque and adventitial neovascularization in an experimental animal model of advanced atherosclerosis and to correlate the in vivo observations with a systematic histological assessment of neovessel density and plaque composition.

METHODS

Experimental design. Aortic atherosclerosis was induced in New Zealand white male rabbits (n = 21) by a combination of 0.2% cholesterol-rich diet and aortic balloon endothelial injury. Six age-matched animals maintained on normal chow served as control subjects. At the end of the atherosclerosis induction, all animals underwent standard and CEU imaging of the aorta, using a crossover design. The animals were randomized to initial ultrasound imaging with either sonographic contrast or saline, and after an interval of 48 h, the studies were repeated using the other agent (saline/contrast). On completion of the imaging studies, the rabbits were euthanized and their aortas processed for histopathology. The study protocol was approved by the Institutional Animal Care and Use Committee.

Atherosclerosis induction. Atherosclerosis was induced using a previously described protocol (17,18). Briefly, male New Zealand white rabbits (3.9 ± 0.5 kg) were fed a 0.2% cholesterol atherogenic diet (Research Diets Inc., New Brunswick, New Jersey) for 9 months. At 12 and 24 weeks of atherogenic diet initiation, aortic balloon endothelial denuditions were performed with a 3- to 4-F Fogarty catheter (Edwards Lifesciences, Irvine, California) under fluoroscopic guidance. The femoral artery was carefully dissected to avoid any nerve damage, and the catheter was progressed until the thoracic descending aorta. The balloon was gently inflated and pulled back until the iliac bifurcation. This procedure was repeated 3 times. Subsequently, the catheter was removed and the femoral artery closed. Anesthesia for the aortic denuditions and imaging process was induced by intramuscular injection of ketamine (30 mg/kg) and xylazine (2.2 mg/kg). Imaging studies were performed as described in the following ultrasound imaging section. After completion of the imaging studies, animals were euthanized by pentobarbital overdose (75 mg/kg, Sleepaway, Fort Dodge, Fort Dodge, Iowa), and the aortas were harvested and processed for histopathology. All animals received humane care in compliance with the Guidelines for the Care and Use of Laboratory Animals.

ABBREVIATIONS AND ACRONYMS

CE = contrast enhanced

CEU = contrast-enhanced ultrasound

Ultrasound imaging. Ultrasound imaging was performed (Philips iEE33 ultrasound machine, Philips, Bothell, Washington), using a 15-MHz linear probe. Image sequences were not electrocardiography gated and the second harmonic detection technique was used for signal detection. First, the infrarenal abdominal aorta was imaged and the plaques localized at the far (posterior) wall of the vessel were selected. This anatomic landmark allowed for a more accurate identification of the selected plaques in the second ultrasound examination as well as for histopathology, using renal

arteries as anatomic landmarks. This criterion was not a limitation in identifying atherosclerotic plaques because all the atherosclerotic rabbits showed plaques at the infrarenal tract. Each plaque was classified according to its echogenicity during ultrasound imaging, using a conventional classification scheme reported previously (15): class I = uniformly echolucent; class II = predominantly echolucent; class III = predominantly echogenic; class IV = uniformly echogenic; and class V = extensive calcification with acoustic shadows.

After standard ultrasound imaging, animals underwent CEU imaging of previously identified lesions using saline or contrast agent. The sonographic contrast agent perflutren lipid microspheres (Definity, Bristol-Myers Squibb Medical Imaging, North Billerica, Massachusetts) was intravenously injected (0.2 ml containing 2.4×10^9 perflutren lipid microspheres) via the marginal ear vein and flushed with 1 ml of saline. Image settings were adjusted to maximize contrast signal visualization and a low mechanical index was used (0.06 to 0.08). A preliminary study was performed to establish the most favorable dose and administration as well as optimization of image settings. The studies were digitally stored for subsequent analysis. Standard and contrast-enhanced images were reviewed offline by 2 readers (E.B., F.F.).

During CEU examinations, plaques appeared dark and hypoechoic because of tissue signal suppression. The movement of the echogenic bubbles into the previously identified atherosclerotic lesions generated moving bright spots within the adventitia and the core of the plaque. According to plaque contrast-agent enhancement, each lesion was categorized either as CE negative (no signal within the plaque or confined to plaque adventitial side) or CE positive (signal reaching the plaque core and/or extensive contrast agent enhancement throughout the lesion), as previously described (15).

Contrast signal enhancement was quantified by a customized semiautomatic analysis program (MATLAB, The MathWorks, Inc., Natick, Massachusetts). The regions of interest, including plaque and adventitia, were set in the ultrasound B-mode images, in a sequence of 10 images before and after contrast/saline injection. Mean gray scale of the images pre- (baseline) and post-injection was calculated and contrast-enhancement expressed as the percentage of increase of mean gray scale versus baseline (pre-infusion) image. Interobserver variability data for the lesion classification was 5% and for the quantitative data was 6%.

Histopathology and immunohistochemistry. After the final imaging session, the animals were euthanized and the abdominal aorta perfused with phosphate-buffered saline 1× and fixed in 4% paraformaldehyde in phosphate-buffered saline as previously described (17,19). Briefly, the infrarenal aortic tract that was analyzed by CEU imaging was cut into 3-mm thick cross sections and embedded in paraffin. Serial sections (5-μm thick) were obtained and stained with combined Masson elastin stain and hematoxylin and eosin. Additional serial sections were assessed for macrophage and smooth muscle cell density by using specific antibodies against RAM-11 (1:100 dilution, Dako, Carpenteria, California) and α-actin (1:100 dilution, Sigma-Aldrich, St. Louis, Missouri), respectively. Isolectin B4 (1:100 dilution, Vector Laboratories, Burlingame, California), staining was performed for characterization and quantification of neovessels. Negative controls were obtained omitting the primary antibodies.

Planimetric analysis of the cellular composition of the lesions was performed using a computer-based quantitative color image analysis system (Image-Pro Plus, MediaCybernetics, Bethesda, Maryland) to assess the percentage of the RAM-11– and α-actin–stained area for each section. The macrophage and smooth muscle cell density of atherosclerotic plaques were quantified and expressed as the percentage of plaque area. The number of neovessels was counted and related to the cross-sectional plaque area. Neovessel density (n/mm^2) was used for correlation with imaging data.

Statistical analyses. Data are presented as mean ± SD or as median with minimum and maximum if not normally distributed. Test of normality was performed using Kolmogorov-Smirnov and Shapiro-Wilk tests. One-way analysis of variance was used to compare differences between groups. The Kruskal-Wallis test was used as appropriate to compare differences between groups for not normally distributed variables (contrast enhancement at computerized analysis, RAM-11). Pearson correlation was applied for linear association between contrast enhancement and intraplaque neovascularization.

RESULTS

CEU imaging. Atherosclerotic lesions at the infrarenal tract of aorta were detected in all the animals

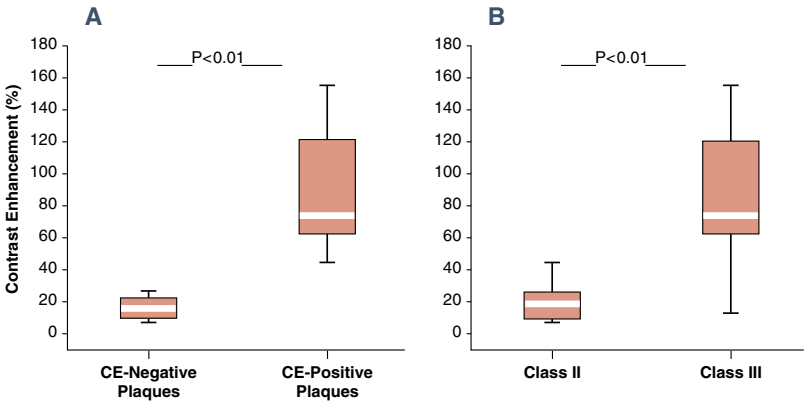

Figure 1. Contrast Enhancement at Computerized Analysis in Atherosclerotic Plaques Classified According to the Visual Contrast Enhancement and Echogenic Class

(A) Plaques classified as contrast-enhanced (CE) plaques at visual analysis showed a higher intraplaque enhancement at computerized analysis compared with CE-negative lesions. **(B)** Class II predominantly echolucent showed less contrast enhancement at computerized analysis compared with class III predominantly echogenic lesions.

using standard ultrasound examination. A total of 21 lesions were identified. Eight plaques (38%) were classified as class II (predominantly echolucent), whereas the remaining 13 lesions (62%) were categorized as class III (predominantly echogenic) (15). No atherosclerotic plaques were detected in the control unmanipulated animals.

After administration of the contrast agent, the aortic lumen appeared opaque for approximately 1 min in both normal and atherosclerotic rabbits. Atherosclerotic lesions, dark and hypoechoic before contrast agent injection, became bright and visible 30 to 60 s later due to the penetration of contrast within the lesion and remained visible for up to 5 min. Observed contrast enhancement was represented by moving bright spots within the plaque (Online Video 1). In contrast, no signal enhancement was evident in control (nonatherosclerotic) animals. No lesions were apparent after saline administration in atherosclerotic animals. Images obtained with CEU were used to classify lesions into CE positive (53%) or CE negative (47%) by visual examination. CE-positive lesions showed a greater plaque enhancement when evaluated by the semiautomated computerized analysis compared with CE-negative plaques (Fig. 1A). Lesions classified as class III (predominantly echogenic) displayed a significantly higher contrast enhancement compared with class II or predominantly echolucent lesions (Fig. 1B). No contrast enhancement, by either visual or computerized analysis, was observed in control animals.

Correlation between histology and CEU imaging. Histological analysis showed no significant differences in plaque size between the CE-positive and CE-negative lesions (Fig. 2A). However, CE-positive lesions were

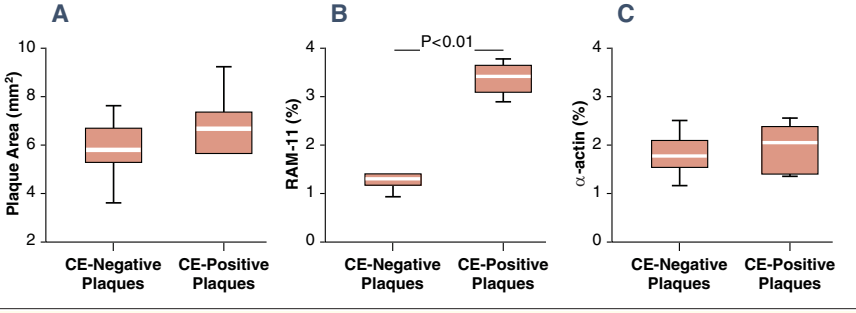

Figure 2. Histological Characterization of Atherosclerotic Lesions Classified According to Visual Contrast Enhancement

(A) Plaque area was similar in both contrast-enhanced (CE) and non-CE lesions. **(B)** A significantly higher content of RAM-11–positive cells (macrophages) were detected in CE than in non-CE lesions. **(C)** In contrast, the amount of α-actin–positive cells (smooth muscle cells) was similar in both type of lesions.

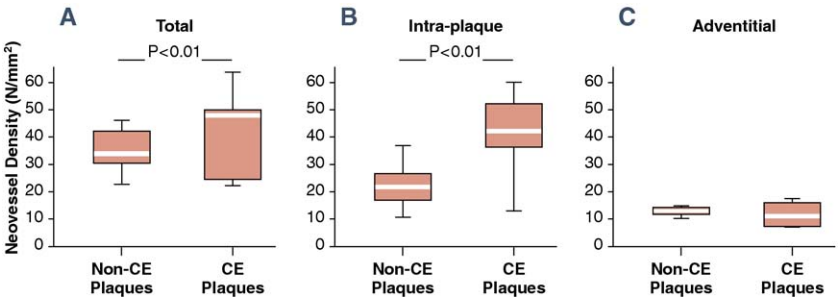

Figure 3. Neovessel Density in Atherosclerotic Lesions Classified According to Visual Contrast Enhancement

(A) The total number of vessels was significantly higher in contrast-enhanced (CE) than in non-CE atherosclerotic lesions. The increased contrast enhancement was related to increased intraplaque neovascularization as demonstrated by the higher intraplaque **(B)**, but not adventitial **(C)**, neovessel density in CE- versus non-CE plaques.

associated with a significantly higher density of macrophages (RAM-11–positive staining) than the CE-negative ones (Fig. 2B). On the other hand, no difference was observed in the density of smooth muscle cells (α-actin–positive staining) between the 2 groups of lesions (Fig. 2C). Similar results were found when the plaques were categorized according to their echogenic class. No significant difference in plaque area was detected between class II and class III lesions (5.8 ± 1.4 mm^2 vs. 6.6 ± 1.0 mm^2, respectively; $p = 0.1$). In contrast, class III lesions showed a significantly higher content of RAM-11–positive cells ($1.6 \pm 0.8\%$ vs. $3.2 \pm 0.6\%$, respectively; $p < 0.001$); α-actin–positive cell (smooth muscle cells) density was no different between class II and III plaques (1.9 ± 0.4 vs. 1.9 ± 0.5, respectively; $p = 0.9$). Class II lesions showed a significantly higher collagen content than class III plaques ($43.2 \pm 9.8\%$ vs. $31.2 \pm 7.3\%$, respectively; $p < 0.01$); elastin content was similar in both groups ($17.6 \pm 4.4\%$ vs. $17.8 \pm 3.5\%$; $p = 0.9$). Similar findings were detected when lesions were classified according to their contrast enhancement. CE-negative plaques showed a significantly greater collagen content than CE-positive ones ($41.8 \pm 8.5\%$ vs. $30.1 \pm 7.0\%$, respectively; $p < 0.04$), whereas the elastin component was similar in both groups ($18.2 \pm 5.1\%$ vs. $17.9 \pm 6.3\%$; $p = 0.8$).

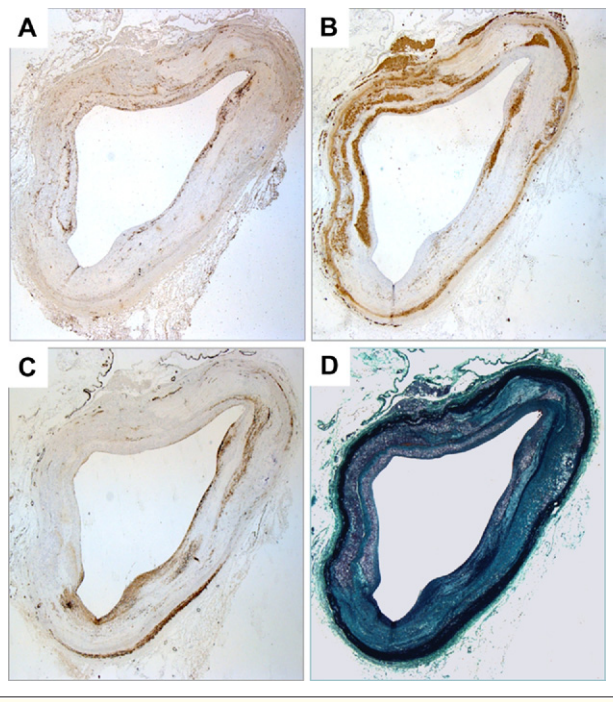

Figure 4. Representative Images Showing CE-Positive Plaque Composition

Contrast-enhanced (CE)–positive lesions showed increased neovessel density **(A)** and increased macrophage infiltration **(B)**. In contrast, smooth muscle cell content **(C)** was similar to that observed in CE-negative lesions. Masson's trichrome staining shows the collagen **(green)** and elastin **(black)** content of CE-positive lesions, which was lower than in CE-negative plaques.

From the imaging view point, an interesting observation was the higher number of neovessels in the arterial wall (adventitia and plaque) in CE-positive lesions compared with the CE-negative lesions (Fig. 3A). A more detailed analysis clearly showed that the difference was mostly due to the increased intraplaque angiogenesis (plaque vasorum) (Fig. 3B); the number of adventitial neovessels was similar among the different lesions (Fig. 3C). These findings are in line with the selected CEU imaging criteria at visual examination defining as CE-positive those lesions with signal contrast agent enhancement within the lesion, and as CE-negative those lesions with no signal within the plaque or confined to the plaque adventitial side.

It is important to note that similar findings were obtained when comparing the cellular composition of the lesions classified according to their echogenic

class. Class III plaques showed a significantly higher total neovessel density compared with class II lesions (40.3 ± 16.0 N/mm^2 vs. 35.7 ± 94.0 N/mm^2, respectively; p = 0.4). These plaques were also associated with a significantly increased plaque-vasorum density than class II lesions (38.1 ± 16.8 N/mm^2 vs. 23.7 ± 7.6 N/mm^2, respectively; p < 0.05). In contrast, adventitial neovessels were similar between class II and III lesions (13.1 ± 1.3 N/mm^2 vs. 11.7 ± 4.0 N/mm^2, respectively; p = 0.3). Figure 4 shows representative images indicating the plaque composition of a CE-positive plaque, characterized by a greater content of macrophages and neovessels. Figure 5 shows representative images of a CE-negative plaque, characterized by a lower neovessel and macrophage density but a greater fibrotic component.

A positive correlation between the number of intraplaque neovessels and contrast signal enhancement of the lesions was noted (Fig. 6). Figures 6A through 6C show the strong contrast enhancement of a CE plaque and the corresponding pathological specimen showing high density of neovessels at immunohistochemistry (Figs. 6E and 6F).

DISCUSSION

We have described the feasibility of CEU imaging for the noninvasive, in vivo visualization of neovascularization in atherosclerotic lesions in a rabbit model of advanced atherosclerosis. The findings were corroborated by histological analyses of the corresponding lesions. The increased plaque angiogenesis associated with macrophage-rich lesions was clearly identified by rapid contrast enhancement of the lesions. On the other hand, more fibrotic lesions with lower macrophage content did not show a similar enhancement. The specificity of the contrast agent used in the study was demonstrated by the lack of lesion enhancement after saline administration in atherosclerotic animals. Similarly, no contrast enhancement in nonatherosclerotic control rabbits after contrast injection was observed.

It is important to outline that the greater neovessel density at histology was observed in CE-positive lesions than in CE-negative lesions. These findings are in agreement with previous data showing a good correlation between vasa vasorum and the degree of contrast agent enhancement in human atherosclerotic lesions (15). However, the atherosclerotic lesions used in that study were highly stenotic because they had to meet the criteria for endarterectomy and therefore did not include lesions with <50% stenosis (20,21). In fact, the high-risk lesions may not always be highly stenotic (22). The use of an animal model of atherosclerosis overrides this limitation, allowing the inclusion of lesions with a greater degree of stenosis. The present study classified lesions not only according to their contrast enhancement but also the histological cellular composition and neovessel density of the imaged lesions.

Interestingly, CEU imaging was able to differentiate plaques according to their vascularization despite their similar sizes. Our results also show a higher macrophage density in CE-positive than in CE-negative plaques, whereas vascular smooth muscle cell density was similar in both groups. Moreover, CE-negative lesions were characterized by a greater fibrotic component than CE-positive plaques. These observations are concordant with those of a previous report showing the relationship between neovascularization assessed by contrast agent enhancement and plaque composition, irrespective of plaque size (15).

Similar results were found when categorizing the atherosclerotic lesions according to their echogenicity. Class III lesions, which showed a significantly

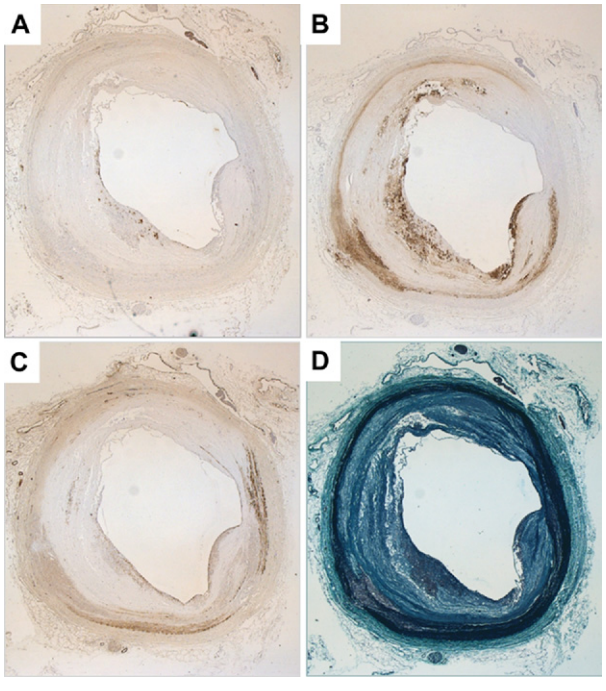

Figure 5. Representative Images Showing CE-Negative Plaque Composition

Contrast-enhanced (CE)–negative lesions showed poor intraplaque neovascularization **(A)** and lower macrophage density **(B)** than CE-positive lesions. Smooth muscle cell content **(C)** was similar to CE-positive lesions. Increased fibrotic component detected by Masson's trichrome staining **(D)** was significantly greater than in CE-positive lesions.

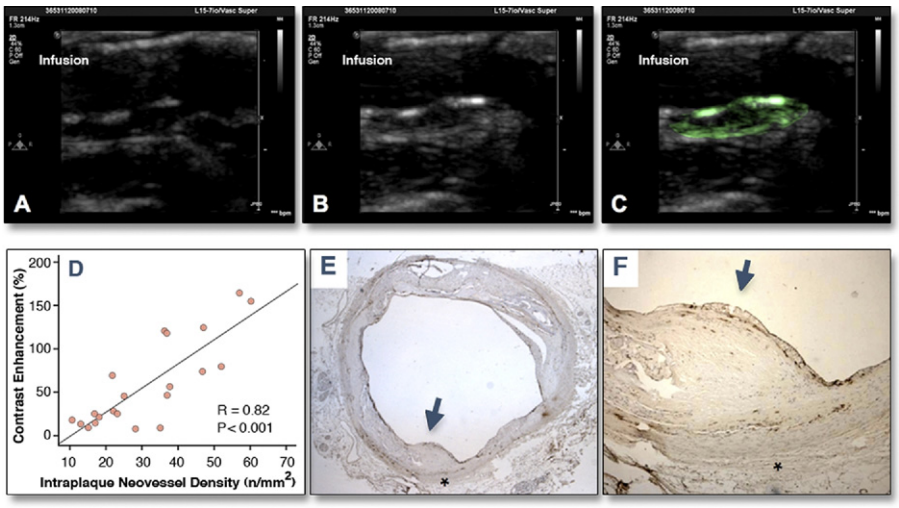

Figure 6. Representative Ultrasound Images of a CE-Positive Atherosclerotic Lesion

Before **(A)** and after **(B)** contrast-administration. **(C)** Contrast enhancement quantification by digital subtraction imaging. **Green area** depicts contrast enhancement of the representative contrast-enhanced (CE)–positive lesion. **(D)** Positive strong correlation between the total number of neovessels and the signal enhancement in fibrofatty lesions is shown. At 25× magnification **(E)** and 200× magnification **(F)**, a histological section of the imaged atherosclerotic plaque stained for lectin (neovessels) is shown. **Asterisk** indicates the corresponding area in the ultrasound images and in the histological section from the same atherosclerotic lesion. **Arrows** in **E and F** indicate the corresponding luminal surface of the plaques in the ultrasound images and in the histological section from the same animal.

greater increase in contrast enhancement compared with class II plaques, demonstrated a similar plaque area but a greater content of macrophages compared with class II lesions. Class III lesions were also characterized by increased neovessel density than class II plaques. These results further confirm that in predominantly echogenic lesions, the increased macrophage density was associated with higher neovessel content, a finding in line with previous observations showing that increased density of intraplaque neovessels is associated with plaque instability (23–25) as well as increased macrophage infiltration (7,15,26). The possibility of directly imaging increased neovascularization may significantly improve plaque characterization over traditional ultrasound. In fact, despite our findings showing that predominantly echogenic lesions also show increased neovascularization and macrophage density, CEU imaging may provide a unique opportunity to monitor the serial progressive pathophysiological developments of intraplaque neovessels (27). Moreover, future application using targeted microbubbles targeting markers of endothelial activation/dysfunction or damage or angiogenesis receptors (28–31) might help to elucidate the mechanism underlying neoangiogenesis in atherosclerosis.

Another novelty of this study concerns the significant association seen between CE-positive lesions and plaque vasorum but not adventitial neovessels compared with CE-negative lesions. These findings suggest that contrast enhancement specifically reflects intraplaque rather than adventitial vascularization. Different results have been reported by others (13,16) describing increased adventitial and intraplaque neovascularization detected by CEU imaging in human carotid atherosclerotic lesions. However, those observations were not corroborated by the systematic histological evaluation of the imaged lesions.

A likely explanation for our findings showing no correlation between contrast enhancement and adventitial neovessels could be related to the speed of penetration of the contrast. Indeed, after contrast injection, the lumen was opacified for about 1 min, not allowing any earlier evaluation of contrast enhancement. Therefore, it is possible that adventitial neovessel enhancement, mostly occurring in this early phase, is actually either underestimated or undetectable. Moreover, a careful adjustment of imaging settings is required to detect contrast agent microbubbles penetrating plaque tissue. After tissue signal suppression, however, the plaque appears dark, allowing easy detection of the microbubbles, the adventitia remains bright, and this could actually limit the detection ability of the technique. Finally, although the experimental animal model used in the present study is characterized by advanced human-like atherosclerotic lesions, as measured by not only lipid content but also by fibrotic areas (17), we cannot rule

out some discrepancy compared with human atherosclerotic lesions.

CONCLUSIONS

The results of the present study support CEU imaging as a feasible technique for the noninvasive assessment of intraplaque neovascularization. Several findings suggest that intraplaque neovascularization is associated with plaque progression and vulnerability (9). Therefore, the availability of a noninvasive technique to assess lesion neovascularization could be of great importance to identify highly vascularized lesions. It has been suggested that inhibition of plaque neovessels could be a potential pharmacological target to promote atherosclerotic lesion stabilization. Therefore, the noninvasive assessment of plaque neovascularization could be of great importance in detecting the presence of highly vascularized lesions and possibly to establish the intensity of antiatherosclerotic treatments (i.e., lipid-lowering approaches).

Acknowledgments

The authors thank Josè Rodriguez, Boris Cortez, and Noemi Escalera for the proper conduct of the experimental work.

Reprint requests and correspondence: Dr. Juan J. Badimon, AtheroThrombosis Research Unit, Cardiovascular Institute, Mount Sinai School of Medicine, One Gustave L. Levy Place, New York, New York 10029. *E-mail: juan.badimon@mssm.edu.*

REFERENCES

1. Ford ES, Capewell S. Coronary heart disease mortality among young adults in the U.S. from 1980 through 2002: concealed leveling of mortality rates. J Am Coll Cardiol 2007;50:2128–32.
2. Carmeliet P. Angiogenesis in health and disease. Nat Med 2003;9:653–60.
3. Moreno PR, Purushothaman KR, Fuster V, et al. Plaque neovascularization is increased in ruptured atherosclerotic lesions of human aorta: implications for plaque vulnerability. Circulation 2004;110:2032–8.
4. Moulton KS. Plaque angiogenesis: its functions and regulation. Cold Spring Harb Symp Quant Biol 2002; 67:471–82.
5. Kolodgie FD, Gold HK, Burke AP, et al. Intraplaque hemorrhage and progression of coronary atheroma. N Engl J Med 2003;349:2316–25.
6. Fleiner M, Kummer M, Mirlacher M, et al. Arterial neovascularization and inflammation in vulnerable patients: early and late signs of symptomatic atherosclerosis. Circulation 2004;110: 2843–50.
7. Kockx MM, Cromheeke KM, Knaapen MW, et al. Phagocytosis and macrophage activation associated with hemorrhagic microvessels in human atherosclerosis. Arterioscler Thromb Vasc Biol 2003;23:440–6.
8. Jeziorska M, Woolley DE. Local neovascularization and cellular composition within vulnerable regions of atherosclerotic plaques of human carotid arteries. J Pathol 1999;188:189–96.
9. Virmani R, Kolodgie FD, Burke AP, et al. Atherosclerotic plaque progression and vulnerability to rupture: angiogenesis as a source of intraplaque hemorrhage. Arterioscler Thromb Vasc Biol 2005;25:2054–61.
10. Heppner P, Lindner JR. Contrast ultrasound assessment of angiogenesis by perfusion and molecular imaging. Expert Rev Mol Diagn 2005; 5:447–55.
11. Feinstein SB. The powerful microbubble: from bench to bedside, from intravascular indicator to therapeutic delivery system, and beyond. Am J Physiol Heart Circ Physiol 2004;287: H450–7.
12. Feinstein SB. Contrast ultrasound imaging of the carotid artery vasa vasorum and atherosclerotic plaque neovascularization. J Am Coll Cardiol 2006;48:236–43.
13. Vicenzini E, Giannoni MF, Puccinelli F, et al. Detection of carotid adventitial vasa vasorum and plaque vascularization with ultrasound cadence contrast pulse sequencing technique and echo-contrast agent. Stroke 2007;38: 2841–3.
14. Shah F, Balan P, Weinberg M, et al. Contrast-enhanced ultrasound imaging of atherosclerotic carotid plaque neovascularization: a new surrogate marker of atherosclerosis? Vasc Med 2007;12:291–7.
15. Coli S, Magnoni M, Sangiorgi G, et al. Contrast-enhanced ultrasound imaging of intraplaque neovascularization in carotid arteries: correlation with histology and plaque echogenicity. J Am Coll Cardiol 2008;52: 223–30.
16. Magnoni M, Coli S, Marrocco-Trischitta MM, et al. Contrast-enhanced ultrasound imaging of periadventitial vasa vasorum in human carotid arteries. Eur J Echocardiogr 2009;10:260–4.
17. Corti R, Osende J, Hutter R, et al. Fenofibrate induces plaque regression in hypercholesterolemic atherosclerotic rabbits: in vivo demonstration by high-resolution MRI. Atherosclerosis 2007;190:106–13.
18. Ibanez B, Vilahur G, Cimmino G, et al. Rapid change in plaque size, composition, and molecular footprint after recombinant apolipoprotein A-I Milano (ETC-216) administration: magnetic resonance imaging study in an experimental model of atherosclerosis. J Am Coll Cardiol 2008; 51:1104–9.
19. Helft G, Worthley SG, Fuster V, et al. Progression and regression of atherosclerotic lesions: monitoring with serial noninvasive magnetic resonance imaging. Circulation 2002;105: 993–8.
20. Biller J, Feinberg WM, Castaldo JE, et al. Guidelines for carotid endarterectomy: a statement for healthcare professionals from a Special Writing Group of the Stroke Council, American Heart Association. Circulation 1998;97:501–9.
21. Chaturvedi S, Bruno A, Feasby T, et al. Carotid endarterectomy—an evidence-based review: report of the Therapeutics and Technology Assessment Subcommittee of the American Academy of Neurology. Neurology 2005;65:794–801.
22. Virmani R, Burke AP, Farb A, Kolodgie FD. Pathology of the vulnerable plaque. J Am Coll Cardiol 2006;47:C13–8.
23. Burke AP, Farb A, Malcom GT, Liang Y, Smialek JE, Virmani R. Plaque rupture and sudden death related to exertion in men with coronary artery disease. JAMA 1999;281:921–6.

24. McCarthy MJ, Loftus IM, Thompson MM, et al. Angiogenesis and the atherosclerotic carotid plaque: an association between symptomatology and plaque morphology. J Vasc Surg 1999; 30:261–8.
25. Mofidi R, Crotty TB, McCarthy P, Sheehan SJ, Mehigan D, Keaveny TV. Association between plaque instability, angiogenesis and symptomatic carotid occlusive disease. Br J Surg 2001;88:945–50.
26. Moreno PR, Falk E, Palacios IF, Newell JB, Fuster V, Fallon JT. Macrophage infiltration in acute coronary syndromes. Implications for plaque rupture. Circulation 1994;90:775–8.
27. Staub D, Schinkel AF, Coll B, et al. Contrast-enhanced ultrasound imaging of the vasa vasorum: from early atherosclerosis to the identification of unstable plaques. J Am Coll Cardiol Img 2010;3:761–71.
28. Villanueva FS, Jankowski RJ, Klibanov S, et al. Microbubbles targeted to intercellular adhesion molecule-1 bind to activated coronary artery endothelial cells. Circulation 1998;98:1–5.
29. Kaufmann BA, Sanders JM, Davis C, et al. Molecular imaging of inflammation in atherosclerosis with targeted ultrasound detection of vascular cell adhesion molecule-1. Circulation 2007;116:276–84.
30. Behm CZ, Kaufmann BA, Carr C, et al. Molecular imaging of endothelial vascular cell adhesion molecule-1 expression and inflammatory cell recruitment during vasculogenesis and ischemia-mediated arteriogenesis. Circulation 2008;117:2902–11.
31. Barreiro O, Aguilar RJ, Tejera E, et al. Specific targeting of human inflamed endothelium and in situ vascular tissue transfection by the use of ultrasound contrast agents. J Am Coll Cardiol Img 2009;2:997–1005.

Key Words: angiogenesis ■ aorta ■ atherosclerosis ■ contrast-enhanced ultrasound imaging.

APPENDIX

For a supplemental video, please see the online version of this article.